Engineering Structures 189 (2019) 359–372

Feasibility study of a hybrid FRP-steel cable-stayed pedestrian swing bridge

Cristiano Alocci [a], Paolo S. Valvo [a,*]

[a] *Department of Civil and Industrial Engineering, University of Pisa, Largo Lucio Lazzarino, I-56122 Pisa, Italy*

Abstract

The paper illustrates the feasibility study of a cable-stayed, pedestrian, swing bridge crossing the Navicelli Canal in Pisa, Italy. The static scheme of the bridge is asymmetric with one tower and three pairs of stays. The maximum span length is 21.26 m and the useful width is 2.50 m. According to the proposed design, the bridge deck will be made of glass fibre-reinforced polymer pultruded profiles; the tower and stays will be of ordinary steel; stainless steel bolts and plates will be used for the connections. A finite element model of the bridge was developed to analyse its structural behaviour during construction, service life, and maintenance operations. Construction stages – with particular attention to the cable stringing procedure – were carefully studied to help reduce the overall deformability of the bridge. Structural verifications were carried out according to the EuroComp Design Code, Italian CNR instructions, and German DIBt specifications. The calculated total weight of the bridge deck is about 11 t, including non-structural elements. Thanks to the low self-weight of the deck, a 3 kW electric motor will be sufficient for movement, with savings in both installation and operational costs with respect to a full steel bridge.

Keywords: Fibre-reinforced polymer; Pultruded profile; Cable-stayed bridge; Pedestrian bridge; Swing bridge.

1. Introduction

Fibre-reinforced polymer (FRP) composite materials have been used for decades in aerospace, mechanical, and naval engineering. In recent years, an increasing number of applications in civil engineering have been realised for the refurbishment of existing structures, as well as for new constructions [1] [2]. In civil engineering, glass fibre-reinforced polymers (GFRP) are mostly used, while the more expensive carbon fibre-reinforced polymers (CFRP) are limited to special applications, where very high structural performances are required (*e.g.*, the strengthening of reinforced concrete or steel structures with pre-stressed laminates [3] [4] [5]). Commonly used matrix materials include polyester, vinylester, and epoxy resins.

FRP materials offer several advantages with respect to traditional construction materials, such as low density (about 1800 kg/m^3), high corrosion resistance, low electrical conductivity,

* Corresponding author. Tel.: +39 050 2218223
E-mail address: p.valvo@ing.unipi.it (P.S. Valvo).

https://doi.org/10.1016/j.engstruct.2019.03.087
Received 16 August 2018; Received in revised form 20 February 2019; Accepted 25 March 2019

and electromagnetic transparency. Their characteristic tensile strength is of the same order of magnitude of the strength of steel profiles (for GFRP, 170–240 N/mm^2). The main disadvantages of FRPs are their low fire resistance and proneness to several damage phenomena and complex failure modes [6]. Moreover, GFRPs are characterised by low elastic modulus (about 1/8 of the Young's modulus of steel), which causes large displacements and significant buckling phenomena. Due to their lightness and slenderness, FRP structures may be sensitive to aeroelastic buckling too.

In the construction sector, the most common technique for the manufacture of structural elements is pultrusion [7]. Pultrusion enables low-cost, large-scale production of rectilinear profiles with generic cross sections (usually, mimicking standard steel profiles) and virtually no length limitation. Conversely, curvilinear elements cannot be obtained by pultrusion, which may be an issue when curved shapes are required for functional or aesthetic motivations. Besides, albeit in theory it would be possible to tailor the cross section and material properties, in practice it is advisable to choose among the commercially available products for both economic concerns (installation costs) and technical reasons (rules for acceptance). Some of the abovementioned disadvantages can be overcome by using vacuum-assisted resin infusion to manufacture the structural elements. Infusion technique was initially limited to small-scale production of special pieces and prototypes [8] [9]. More recently, infusion has been successfully used also in bridge construction. Examples of bridge structures made via infusion process are presented in the review by Smits [10] and in some recent papers by Chróścielewski *et al.* [11] and Siwowski *et al.* [12] [13]. Besides its limitations, infusion has also many advantages, such as the repeatability of production, fast manufacturing, and lack of joints.

FRP bridges have great advantages and potentials with respect to bridges made of traditional materials. On the structural side, they distinguish themselves because of their lightness, ease of assembly, and corrosion resistance. On the economic side, they are competitive both in the construction and maintenance phases. In addition, movable FRP bridges, because of their low self-weight, require less powerful machinery, with consequent cost savings. Thanks to these advantages, an increasing number of all-FRP bridges, as well as hybrid FRP-concrete and FRP-steel bridges, have been built during the last two decades. Examples include mostly pedestrian and cycle bridges [14], but also many highway bridges [15] [16] [17] [18]. Lightweight FRP bridges are also suitable as temporary structures for emergency purposes [19] [20] [21].

The main static schemes used for all-FRP bridges are truss and beam structures. In truss

bridges, usually small-sized profiles are employed and even the parapets are exploited as primary structural components (*e.g.*, the Pontresina Bridge [22]). Beam bridges are common in highway applications, due to their high stiffness obtained by big-sized flanked profiles (*e.g.*, the Route 601 bridge [17]). Their main disadvantage is the sensibility to lateral torsional buckling phenomena, which are significant because diaphragms cannot be placed in the middle of a span.

Hybrid FRP-steel bridges include tied-arch, suspension, and cable-stayed bridges with FRP deck and steel ties. In suspension bridges, often also the towers are made of steel (*e.g.*, the Willcot suspension bridge [23]). In cable-stayed bridges, either steel or FRP is used for the stays. The longest FRP cable-stayed bridge is the Aberfeldy footbridge, which spans 63 m for a total length of 113 m [24]. As will be further discussed below, cable-stayed FRP bridges require some special attention in the design of the cable stringing procedure.

The paper illustrates the feasibility study of a hybrid FRP-steel, cable-stayed, pedestrian, swing bridge crossing the Navicelli Canal in Pisa, Italy. The static scheme of the bridge is asymmetric with one tower and three pairs of stays. The maximum span length is 21.26 m and the useful width is 2.50 m. According to the proposed design, the bridge deck will be made of GFRP pultruded profiles; the tower and stays will be of ordinary steel; stainless steel bolts and plates will be used for the connections. The swinging movement will be obtained by means of a rotating basement, a clamping displacement recovery device, and two carts with crane wheels. Construction stages – with particular attention to the cable stringing procedure – were carefully studied to help reduce the overall deformability of the bridge.

A finite element model of the bridge was developed. Non-linear static analysis was performed for the assembly and cable stringing stage; the stiffness matrix obtained from this analysis was then used for all subsequent dynamic and static analyses. Dynamic modal analyses considered both the closed and open configurations (corresponding to the bridge open and closed to traffic, respectively). Static analyses took into account all of the actions prescribed by current European and Italian regulations. For comparison purposes, structural verifications were carried out according to the EuroComp Design Code [25], Italian CNR instructions [26], and German DIBt specifications [27]. To this aim, a dedicated software tool was developed, which automatically post-processes the finite element analysis results.

The main advantage of the proposed lightweight FRP solution lies in the drastic simplification of the swinging machinery with respect to a traditional steel bridge. The calculated total weight of the bridge deck is about 11 t, including non-structural elements. Thanks to this light weight, a 3 kW electric motor will be sufficient for the bridge movement

with consequent savings in both installation and operational costs. Also, it will not be necessary to use a counterweight to balance the asymmetric spans during opening. Further innovation is in the proposed mounting plan and cable stringing procedure, which help reduce the deformability of the finally assembled structure.

To the best of the Authors' knowledge, the planned bridge would be the first example of cable-stayed swing bridge with all-FRP deck. Further details about the project can be found in the first Author's MSc Thesis [28].

2. Hybrid FRP-steel swing bridge on the Navicelli Canal in Pisa

2.1. General description

The planned bridge will cross the *Canale dei Navicelli* (Navicelli Canal) in Pisa, Italy. This is an artificial canal built between 1563 and 1575 to connect the city of Pisa with the seaport of Leghorn [29]. The new bridge will replace an existing temporary floating bridge, thus realising a permanent connection for pedestrians and cyclists between the two banks of the canal. The bridge will close the gap between a recently completed bikeway, running from the city centre to the construction site, and an older pathway, running parallel to the canal for about 16 km up to the intersection with the diversion of the river Arno in Calambrone (Fig. 1)

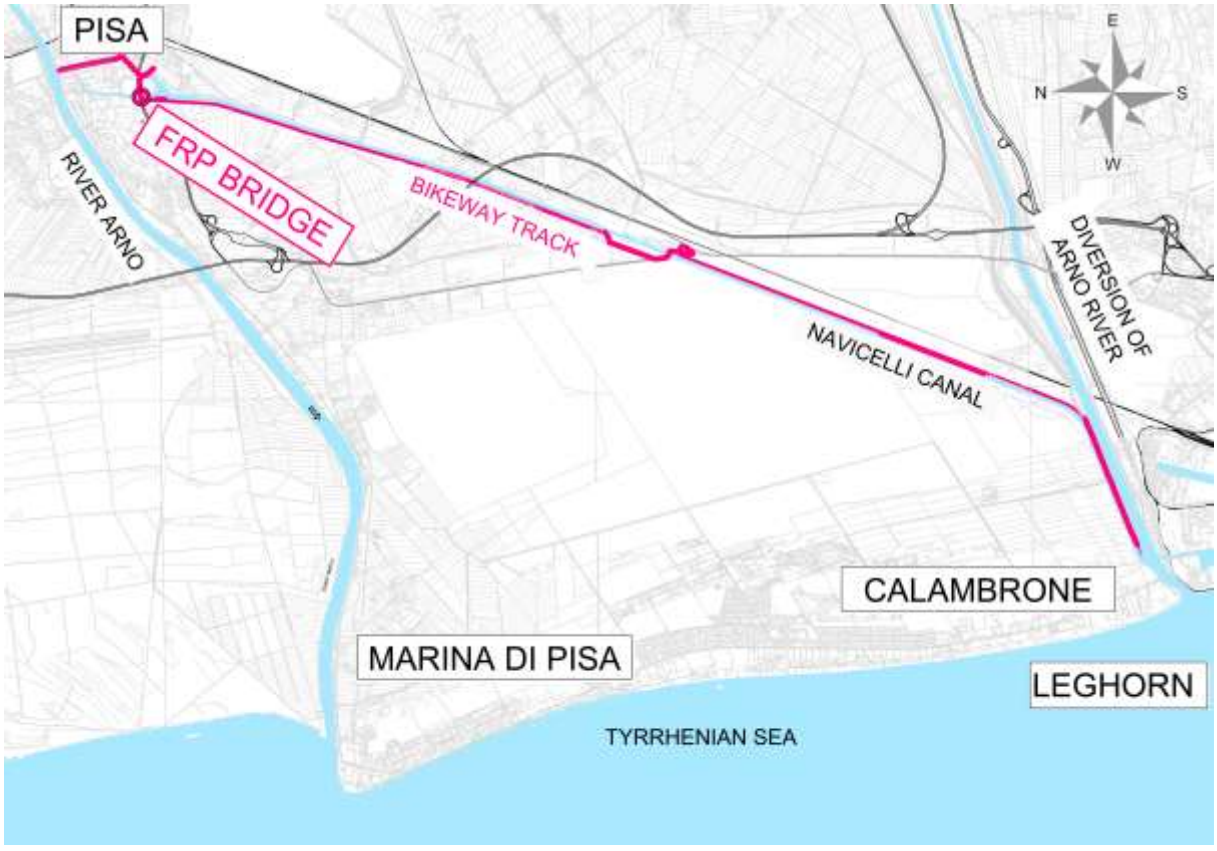

Fig. 1. Location of the bridge.

The Client is the company *Navicelli di Pisa S.p.A.* [30], which manages the canal and the area of the construction site. According to the Client's specifications, the bridge has to be moveable, as not to create interference with maritime traffic on the canal, where shipbuilding activities thrive. Moreover, the Client intends to keep the bridge closed to traffic by night for safety issues. Lastly, the new bridge has to be built adjacent to a viaduct of the Florence-Pisa-Leghorn highway. Therefore, a swinging kinematic mechanism was chosen with an additional abutment on the *Darsena Pisana* (Pisan dock) side (Fig. 2).

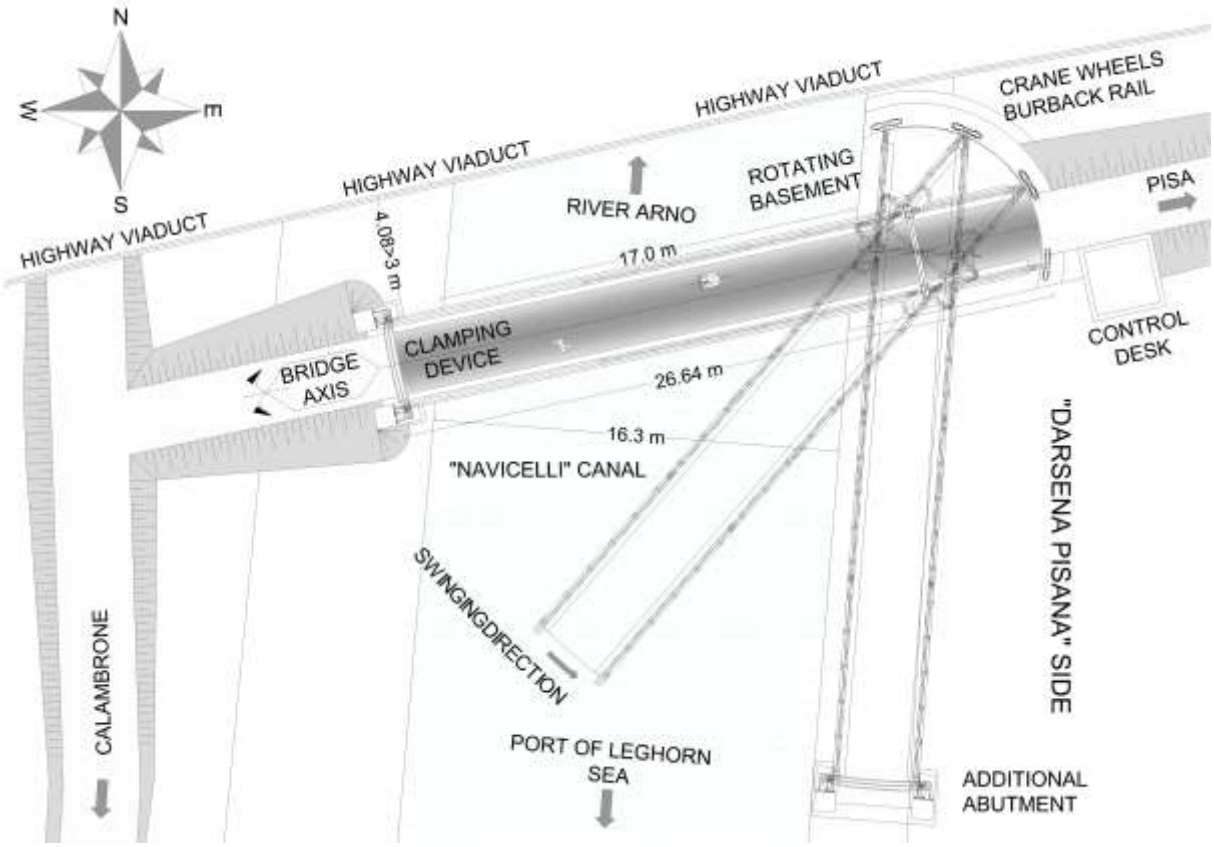

Fig. 2. Plan view of the construction site and kinematics of the swinging mechanism.

The planned structure will be an asymmetric, cable-stayed bridge with one tower and three pairs of stays. The bridge total length will be 26.64 m, the maximum span length will be 21.26 m, and the useful width will be 2.50 m. In order not to create interference with the viaduct, the tower height will be limited to 7.89 m above mean sea level (m.s.l.), *i.e.* 1.04 m below the lower surface of the viaduct (Fig. 3).

The parapets are conceived as plane truss beams and considered as primary structural elements. The parapets are inclined with respect to the vertical plane to enable the anchorage of the stays. The latter are connected directly to the webs of the pultruded profiles used as longitudinal girders (Fig. 4). Such design options were chosen to minimise the stresses in the transverse-to-fibre direction in the girders. In the horizontal plane, the deck has a bracing system for transversal actions (Fig. 5).

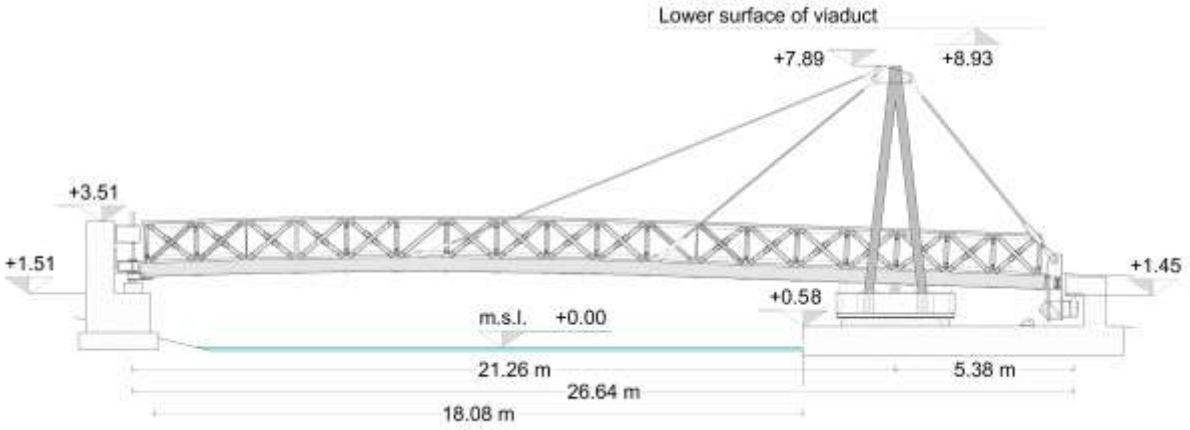

Fig. 3. Side view of the bridge.

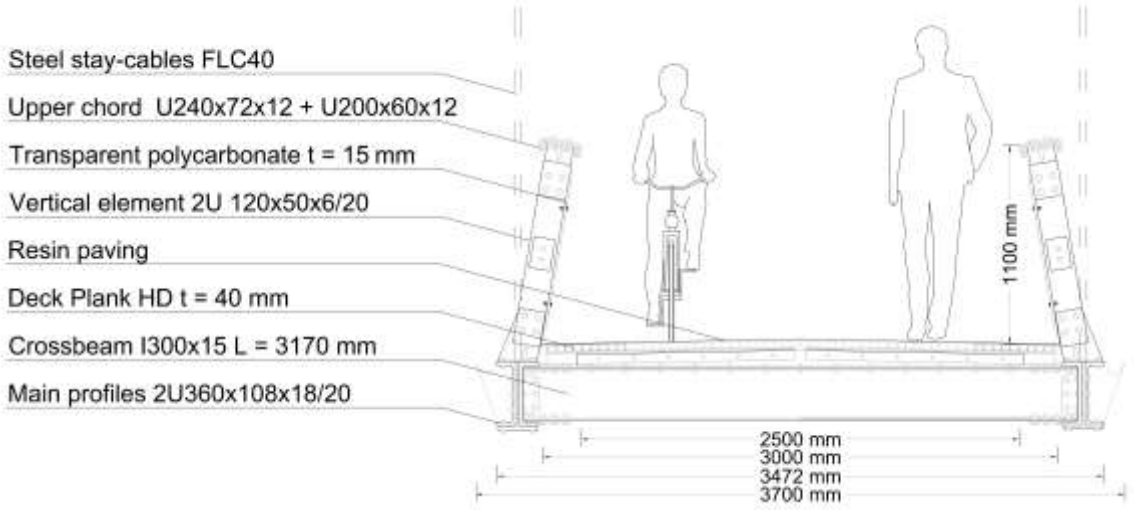

Fig. 4. Cross section of the bridge deck.

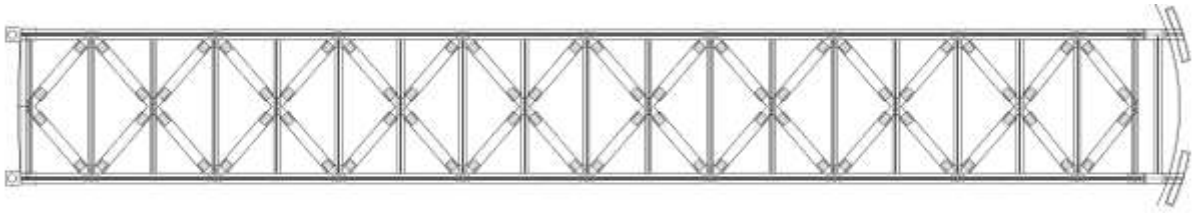

Fig. 5. Horizontal bracing system.

2.2. Materials and structural elements

The bridge deck will be made of GFRP pultruded profiles and planks. The main structural elements will be two longitudinal girders, each having a double channel section 2U 360x108x18/20 (all section sizes are in mm). The upper chords of the parapets will be obtained by joining two profiles with channel sections U 240x72x12 and U 200x60x10 (the second profile inside the first one). The vertical elements and diagonals of the parapets will be profiles with double channel section 2U 120x50x6/20. Some diagonals will be made of stainless steel plates because they cooperate with the stringing system. The horizontal bracing system will be made of profiles with channel section U 240x72x12. Figure 6 represents a 3D

view of a main structural node of the deck, showing the cross sections of the adopted profiles. Figure 7 shows a detail of the connection between the steel stay cables and main GFRP girders. The walking surface of the deck will be made of 40 mm thick plank profiles. Figure 8 shows a detail of the joints between the plank elements and crossbeams. All of the selected elements correspond to standard products by Fiberline Composites A/S [31], reaching the requirements of class E23 according to EN 13706-2:2002 [32]. The design material properties are reported in Table 1.

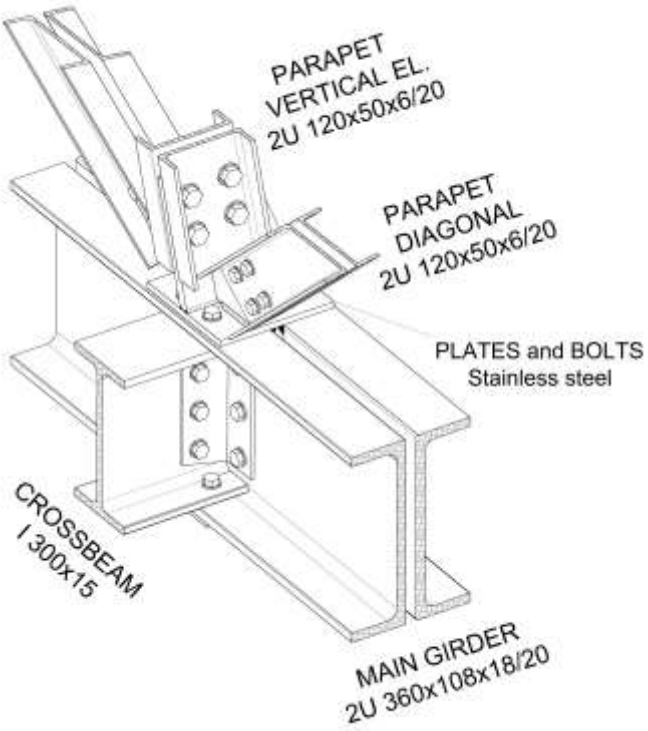

Fig. 6. 3D view of a main structural node of the deck.

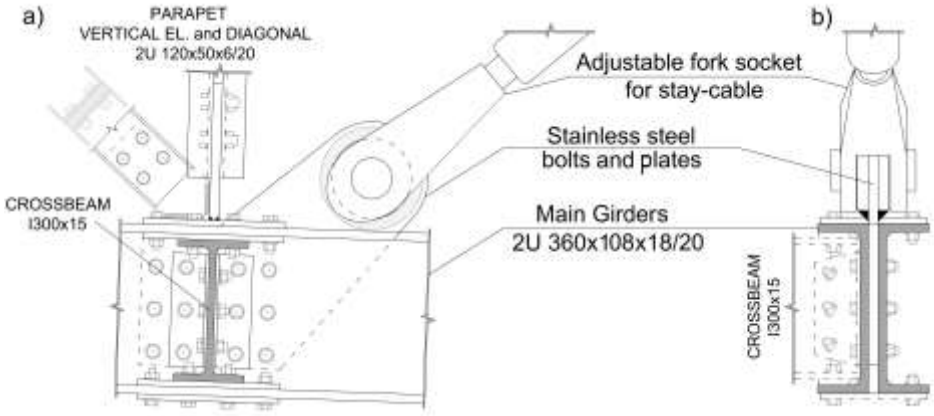

Fig. 7. Detail of the connection between stay-cables and main girders: (a) lateral view; (b) cross section.

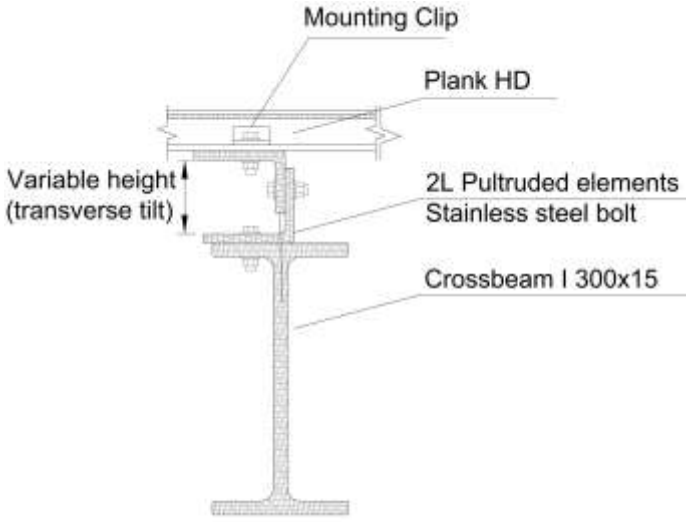

Fig. 8. Detail of joints between plank elements and crossbeams.

Table 1

Material properties of GFRP profiles.

Property	Value
Grade according EN 13706-2:2002	E23
Longitudinal elastic modulus E_x	24000 N/mm^2
Transverse elastic modulus E_y	7000 N/mm^2
Shear modulus G	3000 N/mm^2
Poisson's ratio v_{yx}	0.23
Poisson's ratio v_{xy}	0.07
Longitudinal characteristic strength	240 N/mm^2
Transverse characteristic strength	50 N/mm^2
Interlaminar shear strength	20 N/mm^2
In-plane shear strength	40 N/mm^2
Pin-bearing strength (longitudinal)	200 N/mm^2
Pin-bearing strength (transverse)	120 N/mm^2

The tower will be made of ordinary steel to ensure the required stiffness against vertical and lateral loads, as well as global buckling phenomena. It will be composed by two parts joined by an IPE 600 section profile with a central bolted joint (Fig. 9a). In turn, each part will consist of two inclined profiles with rectangular hollow section RHS 500x300x12.5 (Fig. 9b). The stays will consist of steel full locked coil strands with a diameter of 40 mm. Connections between GFRP elements will use stainless steel bolts and plates. The material properties of all of the steel elements are listed in Table 2.

The design of bolted connections between GFRP elements requires special caution to avoid brittle fracture phenomena, which are very common in composite systems. According to the standards for FRP constructions, the minimum distances between the bolt holes and from holes to edges are greater than for steel structures. In particular, the least external dimension of the washers shall be not less than twice the diameter of the bolts [25] [26] [27]. It is also

necessary to pay attention to avoid stresses in the transverse-to-fibre directions.

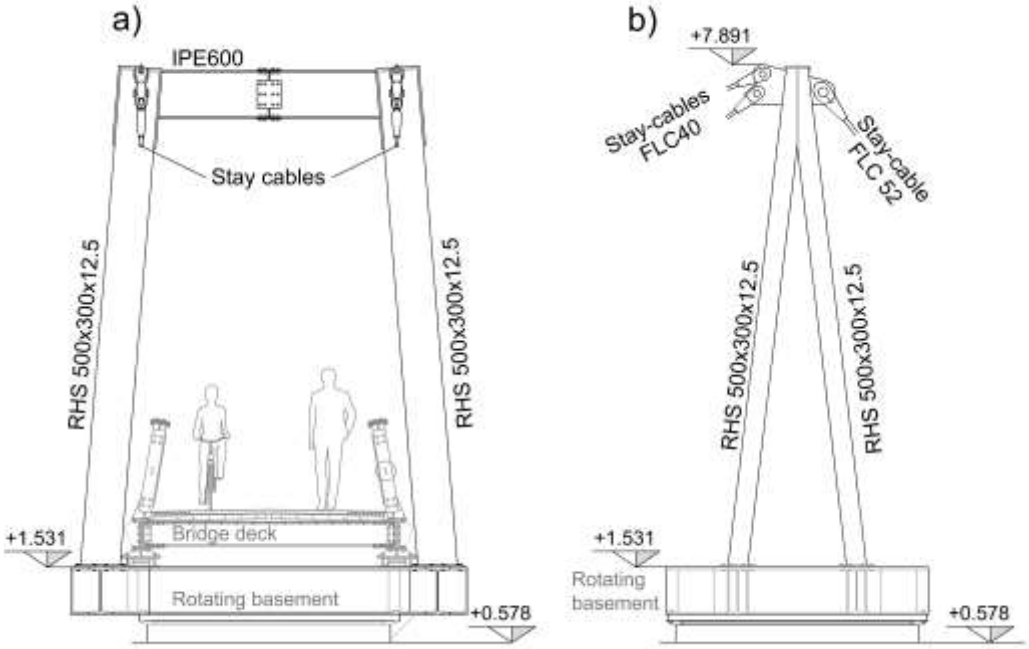

Fig. 9. Steel tower: (a) frontal view; (b) lateral view.

Table 2

Material properties of steel elements.

Item	Type	Standard	Yield strength f_y (N/mm^2)	Ultimate tensile strength f_u (N/mm^2)
Tower and machinery profiles	S275	EN 1993-1-1	275	430
Tower and machinery bolts	Grade 8.8	EN 1993-1-1	640	800
Bridge connection plates	AISI 304	EN 1993-1-4	200	500
Bridge connection bolts	A2/70	EN 1993-1-4	450	700
Stay cables – Full locked coil strands		EN 1993-1-11	–	1490

3. Construction stages

3.1. Mounting plan

The mounting plan consists of the following construction stages:

1. the deck is produced in the workshop subdivided into three segments (Fig. 10a);
2. the concrete abutments are cast in place, then the machinery and bearing devices are placed over the abutments;
3. the straight deck segments are transported to the construction site, where they are first assembled and then placed over the abutments;
4. the vertical elements, upper chords, and a few selected diagonals of the parapets are mounted (Fig. 10b);
5. the tower is installed and the stays are stretched so as to produce a controlled deformation of the deck, as described in the following Section 3.2 (Fig. 10c);

6. the remaining diagonals of the parapets are mounted and finishing touches are given (Fig. 10d).

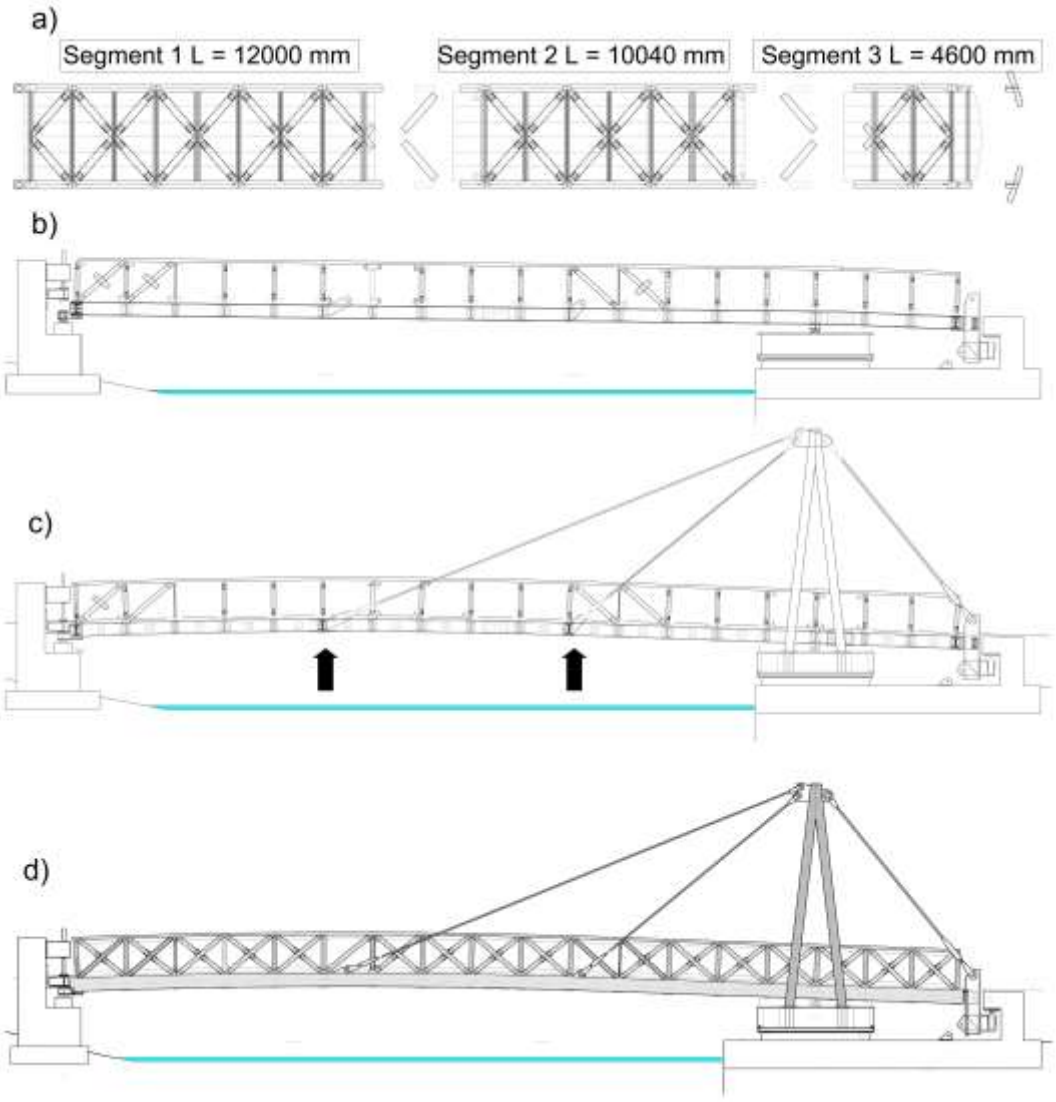

7.

8. **Fig. 10.** Construction stages: (a) plan view of prefabricated deck segments; (b) the deck is assembled on site and the parapets are partially mounted; (c) the tower is installed and the stays are stretched; (d) the parapets are completed with the remaining diagonals and finishing touches are given.

3.2. Cable stringing procedure

A significant design problem with cable-stayed FRP bridges is that, due to the low self-weight of the deck, the stays are weakly stretched and therefore very deformable in the transverse direction because of the Dischinger's effect [33] [34] [35]. Accordingly, the apparent extensional stiffness of an inclined cable is

$$EA^{*} = \frac{EA}{1+\dfrac{(\gamma l_0 A)^2}{12}\dfrac{EA}{N}}, \tag{1}$$

where E and γ respectively are the Young's modulus and weight per unit volume of the material, A and l_0 respectively are the cross section area and horizontal projected length of the cable, and N is the acting axial force.

In existing FRP bridges, the abovementioned problem has been overcome by using composite stays instead of steel cables or adding ballast masses to the deck [24]. However, composite stays are still in the experimental phase and not commercially widespread. Besides, for the present application, additional ballast masses would nullify the benefits from the low self-weight during the opening of the bridge. As an alternative, the proposal is to stretch the stays before completing the installation of the diagonal bars. Additional axial forces will be introduced in the stays after the completion of construction (deck and complete parapets). This particular stringing procedure is deemed to introduce sufficiently high axial forces in the stays and provide the structure with the required overall stiffness.

As an additional benefit, the deformation of the deck will produce a curvilinear road axis in the vertical plane, although the structure will be assembled by using only standard, straight pultruded profiles. In order to approximate the desired curvilinear axis, a manual calibration of the design axial forces in cables was carried out. Furthermore, the upper chords and diagonals of the parapets will be pre-stressed, thus preventing lateral buckling phenomena.

4. Structural design

4.1. Finite element analysis

4.1.1. Model

Structural analysis was performed by using the finite element method (FEM) as implemented into the commercial software code SAP2000 [36]. A model of the bridge (Fig. 11) was set up using a total of 499 one-dimensional FRAME elements, for the GFRP and steel profiles, and CABLE elements, for the stays. The deck was modelled using 576 two-dimensional SHELL elements with nearly zero stiffness. Such elements do not contribute in practice to the global stiffness matrix of the model, but only to its mass matrix. So, to be on the safe side, the weight and mass of the deck are considered, but not its composite action with the girders. Also, the computation of meaningless local modes in modal analysis is avoided.

Joints between profiles were modelled using rigid LINK elements to take into account any eccentricity of the centrelines of the connected elements. A total of 289 rigid elements were used. Bending moment releases were introduced at both ends of FRAME elements representing the parapet profiles to model their truss behaviour. The masses of the steel plates

of bolted connections were explicitly introduced into the model, since they turn out to be non-negligible compared to other structural masses. The external bearings were modelled as linear springs with the nominal stiffness declared by the bearing supplier.

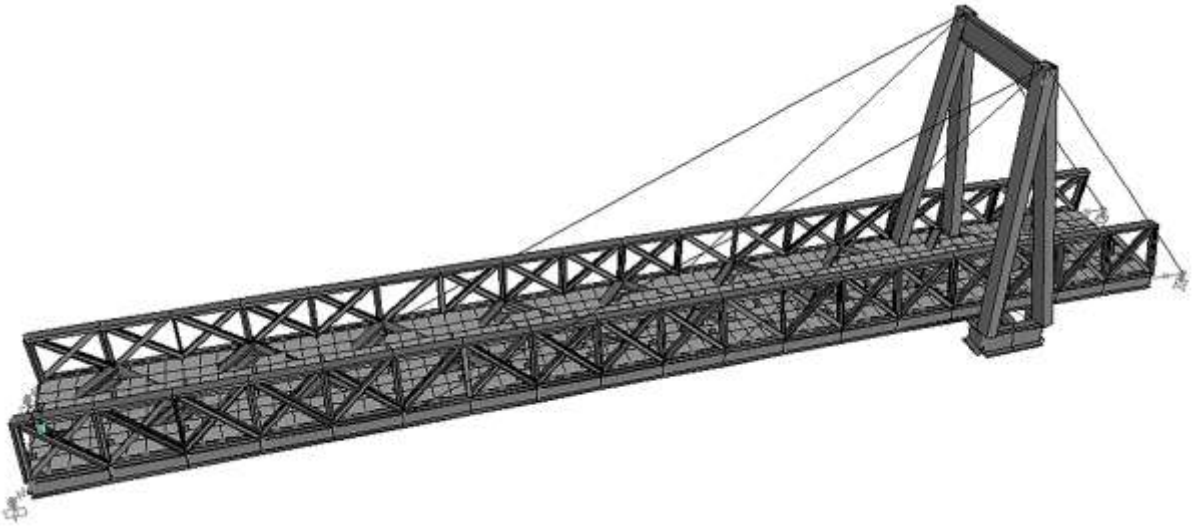

Fig. 11. Finite element model of the bridge.

4.1.2. Analysis

Non-linear static analysis was performed for the assembly and stringing stage. All of the subsequent analyses were conducted assuming linear response, but using the stiffness matrix obtained from the first non-linear analysis. In this case, such an approach is considered to be effective, since the adopted stringing procedure determines a state of stress in the stays that is sufficient to overcome the Dischinger's effect.

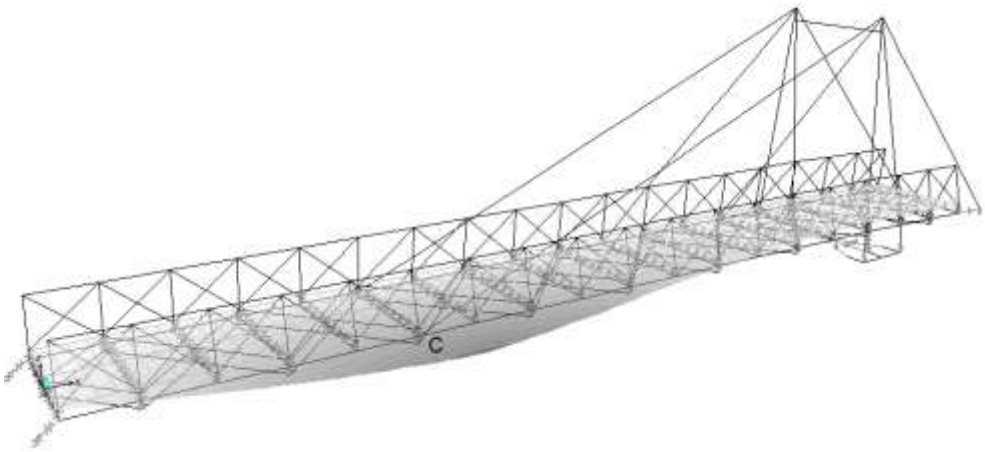

Fig. 12. Influence surface for the vertical displacement at point C.

Dynamic modal analyses were conducted to study the free vibrations of the bridge in both the closed and open configurations. Static analyses considered all of the actions prescribed by the Eurocode 1 Part 2 [37] and Italian regulations [38]: self-weight, pedestrian traffic, wind, snow, thermal actions, creep, earthquake, accidental loads on parapets, and inertial loads due to the swinging movement [28]. In particular, traffic loads were considered as 5.00 kN/m^2

uniformly distributed vertical loads. To maximise their effects, traffic loads were placed on the deck according lane-type influence surfaces (see an example in Fig. 12). Seismic analyses were conducted with behaviour factor $q = 1$, due to the brittle behaviour of GFRP.

4.1.3. Results

Table 3 shows the calculated axial forces, N, and ratios of the apparent vs. nominal extensional stiffness, EA^*/EA, of the cables due to the bridge self-weight. For comparison, the table also shows the results obtained by assuming a standard stringing procedure, where the cables are stretched after the complete assembly of the deck. With the standard stringing procedure, the extensional stiffness ratio turns out to be very low. Instead, with the proposed procedure, the same ratio approaches 100%, which *a posteriori* justifies the adoption of a linearly elastic analysis to model the structural behaviour after the assembly and stringing stage.

Tables 4 and 5 summarise the results of the dynamic modal analyses in terms of the most relevant modes of vibration of the bridge in the closed and open configurations, respectively. Figures 13 and 14 show the corresponding first three mode shapes. In the closed configuration, the frequency of the first flexural mode in the vertical plane (6.36 Hz) is greater than 5 Hz, which is considered sufficient to avoid resonance problems due to pedestrian traffic. In the open configuration, the static scheme of the bridge resembles that of a cantilever beam. The overall behaviour is consequently less stiff and the natural frequencies are lower.

4.2. Structural verifications

4.2.1. Combination of actions and reference guidelines

To conduct the structural verifications, the stresses calculated for the elementary actions were combined according to Italian regulations [38]. In this way, 408 fundamental combinations were obtained, as well as 72 quasi-permanent combinations, 72 seismic combinations, and 30 accidental combinations (24 with accidental loads on parapets and 6 accounting for the breaking of cables) [28].

For comparison purposes, the structural verifications were carried out according to three different guidelines: the EuroComp Design Code [25], Italian CNR instructions [26], and German DIBt specifications [27].

Table 3

Axial forces and extensional stiffness ratios in cables under self-weight.

Stringing procedure	Most inclined cable		Less inclined cable	
	Axial force (kN)	Stiffness ratio (%)	Axial force (kN)	Stiffness ratio (%)
Standard	47.4	21	21.0	8
Proposed	258.9	98	85.5	86

Table 4

Free vibration characteristics of the bridge in closed configuration.

Mode	Period (s)	Frequency (Hz)	Participating mass				Type
			UX (%)	UY (%)	UZ (%)	RX (%)	
1	0.4052	2.47	0	34.350	0	0.357	Flexural (horizontal)
2	0.1572	6.36	0.214	0	36.760	0	Flexural (vertical)
3	0.1362	7.34	0	0	0	6.107	Torsional
4	0.1007	9.93	0	7.468	0	3.246	Flexural / Torsional
6	0.0945	10.58	17.856	0	0	0	Extensional

Table 5

Free vibration characteristics of the bridge in open configuration.

Mode	Period (s)	Frequency (Hz)	Participating mass				Type
			UX (%)	UY (%)	UZ (%)	RX (%)	
1	0.4945	2.02	0	26.345	0	0.443	Flexural (horizontal)
2	0.4540	2.20	0	0	28.389	0	Flexural (vertical)
3	0.2584	3.87	0	8.062	0	9.781	Flexural / Torsional
4	0.1272	7.86	0.763	0	12.185	0	Flexural (vertical)
5	0.1241	8.06	0	4.214	0	0.420	Flexural (horizontal)
7	0.0944	10.59	17.120	0	0	0	Extensional
8	0.0914	10.94	0	4.638	0	0.439	Flexural (horizontal)

Table 6

ULS verification ratios according to different standards.

Verification	Element	Sizing point	EuroComp	CNR	DIBt
Compression	Parapet diagonal	A	0.650	0.711	0.740
Tension	Parapet chord	B	0.322	0.353	0.330
Compression and bending	Principal girder	C	0.810	0.940	0.622
Tension and bending	Principal girder	D	0.362	0.397	0.169

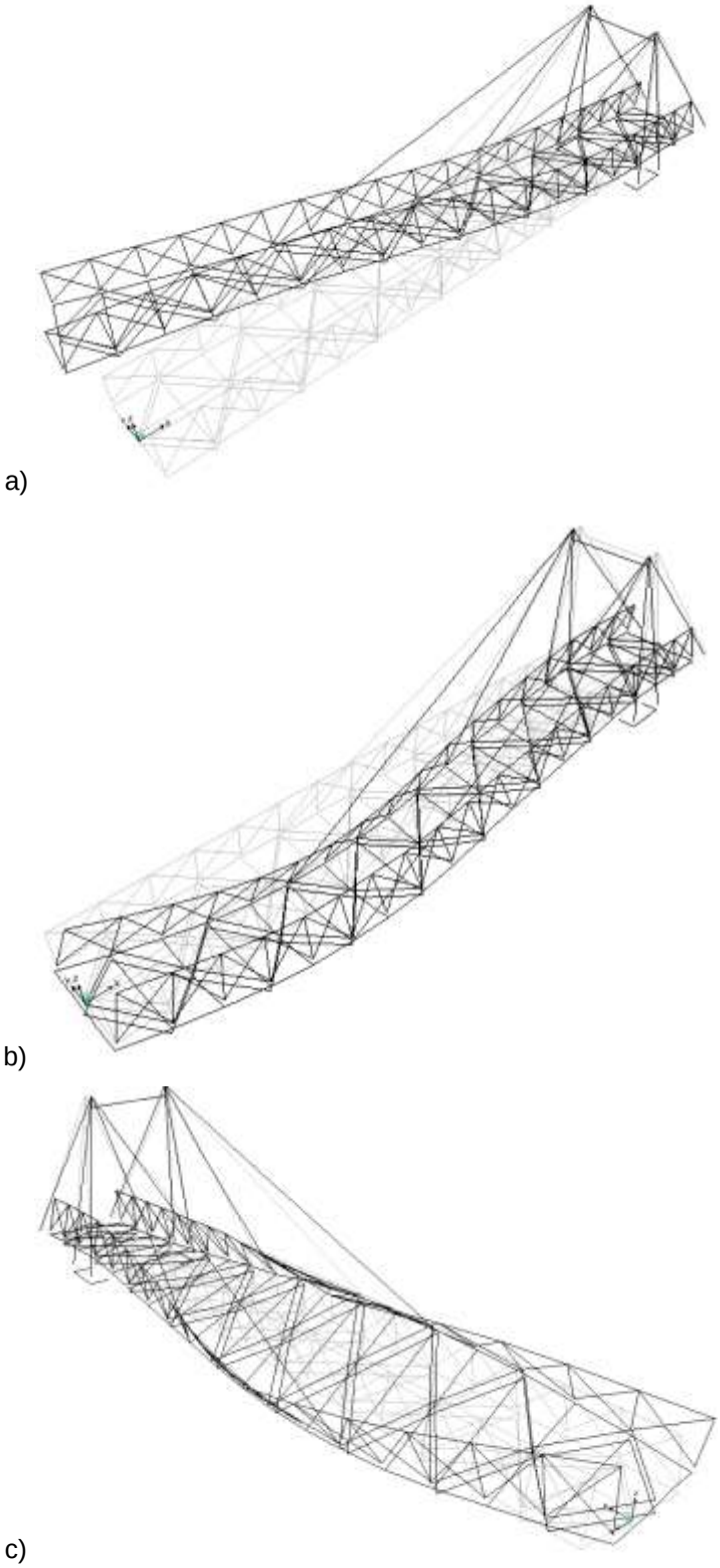

Fig. 13. Mode shapes of the closed bridge: (a) 1st mode; (b) 2nd mode; (c) 3rd mode.

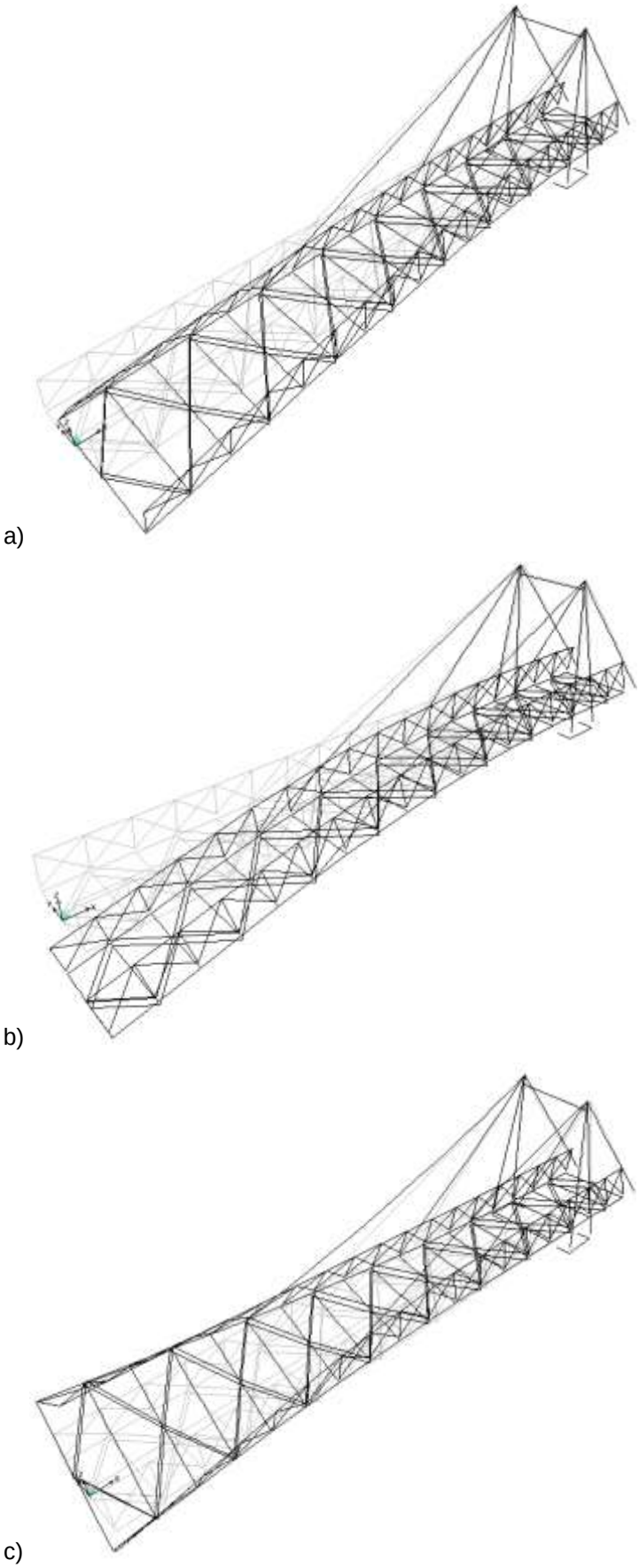

Fig. 14. Mode shapes of the open bridge: (a) 1st mode; (b) 2nd mode; (c) 3rd mode.

4.2.2. Verification software tool

A dedicated software tool was programmed using Visual Basic for Applications (VBA) and Structured Query Language (SQL) to post-process the FEM analysis results. The software tool automatically calculates all of the prescribed combinations of actions. Then, it carries out the requested structural verifications and furnishes output tables in Microsoft Word format (Fig. 15).

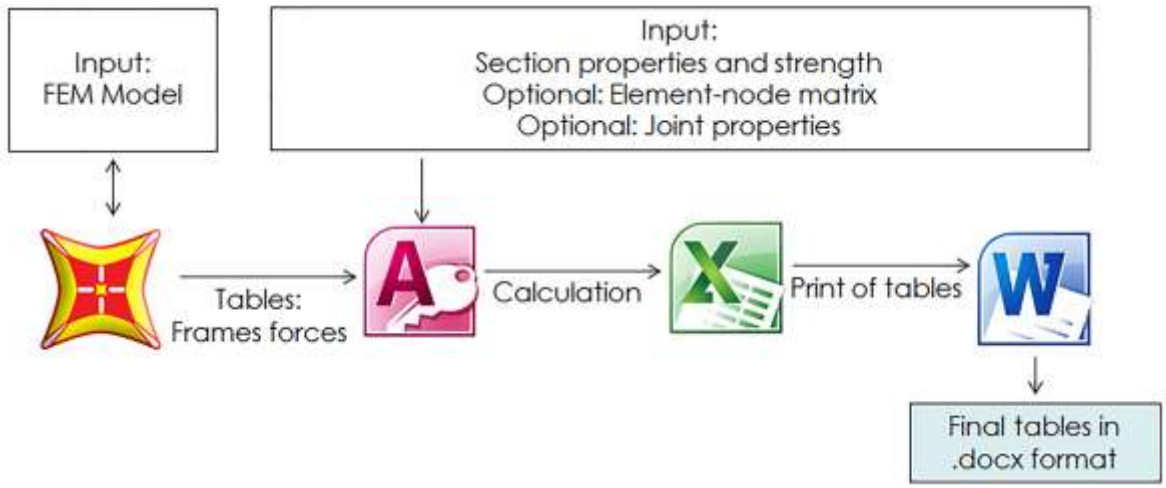

Fig. 15. Verification software tool flowchart.

4.2.3. Results of verifications

In the ultimate limit state (ULS) verifications, the main differences among the compared guidelines lie in the values of some safety coefficients: for example, the material safety coefficient is 1.50 for EuroComp, 1.64 for CNR, and 1.71 for DIBt.

Table 6 reports the maximum calculated verification ratios, defined as the ratios between the design forces (demand) and the corresponding resistances (capacity). These values should all be less than or equal to 1 to be on the safe side. Figure 16 shows the critical points of the structure for the structural verifications.

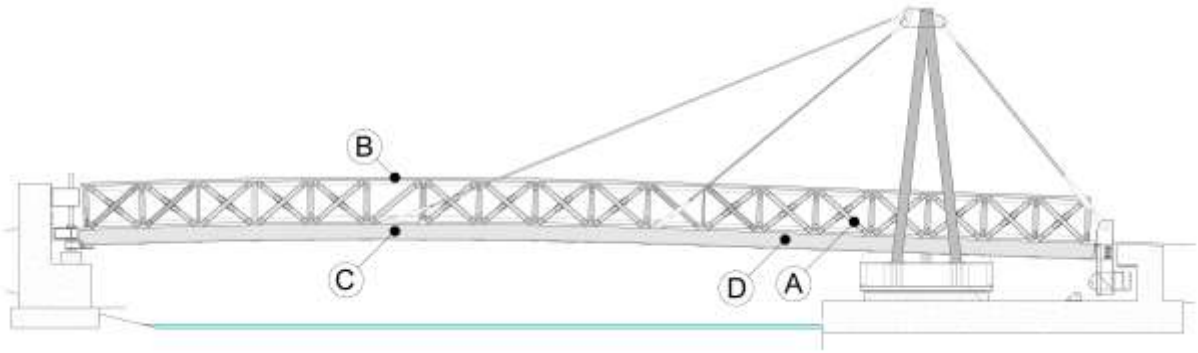

Fig. 16. Sizing points for structural verifications.

The ULS verifications of members in compression furnished similar results among the compared guidelines. The most important limitation of strength was due to the local buckling

of flanges. The ULS verification of members in tension considered the net area of sections. According to DIBt specifications, the verifications against combined compression (or tension) and bending are based on allowable stresses. The resulting verification ratios were lower than those obtained through the other two guidelines. According to CNR instructions, in the verifications against combined compression and bending the safety coefficient is applied twice, for both the calculation of the critical buckling load and final strength. As a result, the calculated verification ratios turned out to be the highest.

For joints, bearing failure is the sizing verification. The geometry limitations are higher than in steel. Minimum hole-to-hole distance and bolt diameter ratio is 4 (2.2 in steel), hole-to-edge distance ratio is 4 (1.2 in steel). Because of the complex geometries of some joints, the lack of interference between bolts and plate accessibility were checked (Fig. 17). CNR instructions are the most conservative, due to a multiplicative row coefficient, which considers the uncertain share of forces between the bolts and the low stiffness of the material.

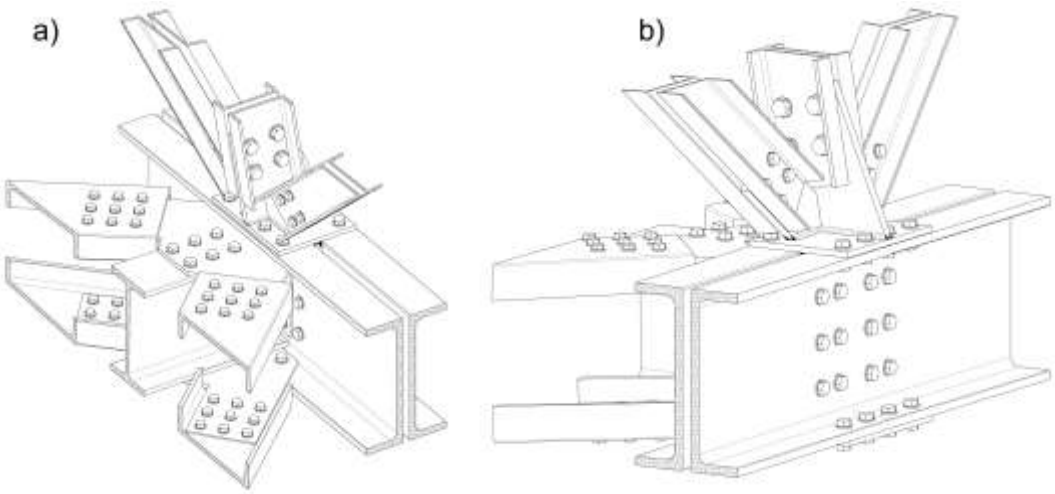

Fig. 17. Verification of the lack of interference between bolts and plate accessibility: (a) internal view; (b) external view.

The serviceability limit state (SLS) verifications included displacement and strain limitations. Maximum values of deflection to span ratio can be found in different references: for instance, CNR-DT 205/2007 instructions [26], DIBt specifications [27], and AASHTO specifications [39]. The more restrictive condition is given by AASHTO specifications (1/400 of span). Instead, strain limitations are suggested by DIBt specifications to prevent excessive creep phenomena.

Because of the lightness and slenderness of the structure, also aero-elastic buckling was checked to prevent vortex shedding and galloping. The verifications were carried out according CNR-DT 207/2008 instructions [40] and Eurocode 1 Part 1-4 [41]. The vortex shedding and galloping critical wind velocities are reported in Table 7. The bridge is more

exposed in the open (moving) configuration, when it behaves globally like a cantilever beam and the stiffening effect of the proposed cable stringing procedure is no longer effective.

Table 7

Vortex shedding and galloping critical velocities.

Configuration	Design return period	Maximum wind velocity		Wind critical velocity	
	T_R (years)	$v_{max}(10\ T_R)$ (m/s) [35]	$1.25\ v_{max}(T_R)$ (m/s) [36]	Vortex shedding v_{cr} (m/s)	Galloping v_G (m/s)
Closed	50	25.51	26.41	61.96	160.37
Open	10	18.00	19.80	21.47	55.57

5. Swinging machinery

The total weight of the bridge deck turns out to be about 11 t, including non-structural elements, which correspond to 167 kg/m^2 of walkable area. This low self-weight enables the use of small-sized machinery, with consequent savings in both installation and operational costs. In particular, a 3 kW electric motor will be sufficient to transmit the required torque to the swinging mechanism.

The estimate opening time is about 3 minutes. The swinging of the bridge begins with the activation of a displacement recovery device, enabling the lifting of the bridge on the abutment. The device consists of a steel load bar moved by two jackscrews that are jointed to steel shelves (Fig. 18). The rotating basement is connected to a slewing bearing with one row of spherical rollers and inner gear teeth (Fig. 19). To ensure the transmission of vertical reactions, carts with crane wheels and a Burback rail are placed at the other end of the bridge (Fig. 20).

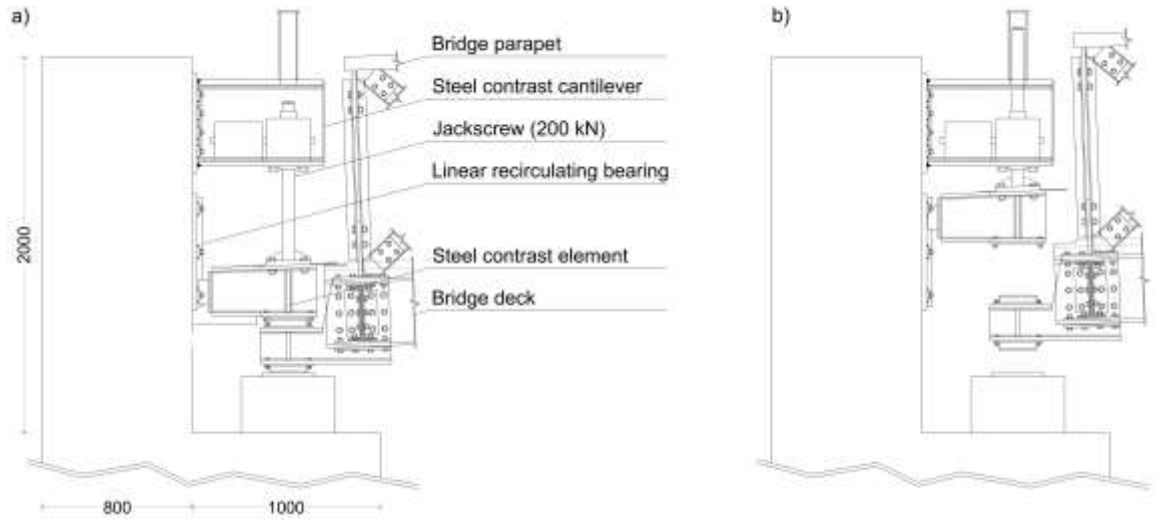

Fig. 18. Clamping displacement recovery device: (a) closed bridge; (b) open bridge.

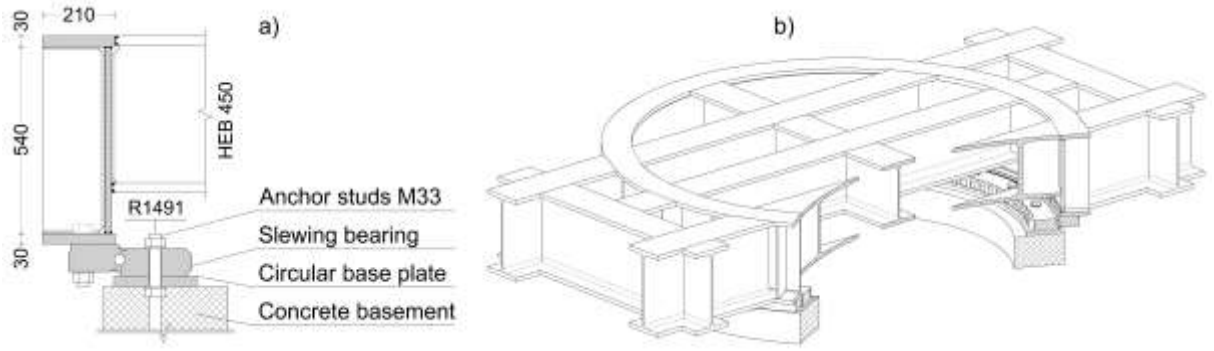

Fig. 19. Rotating basement connected to slewing bearing: (a) lateral view; (b) 3D view.

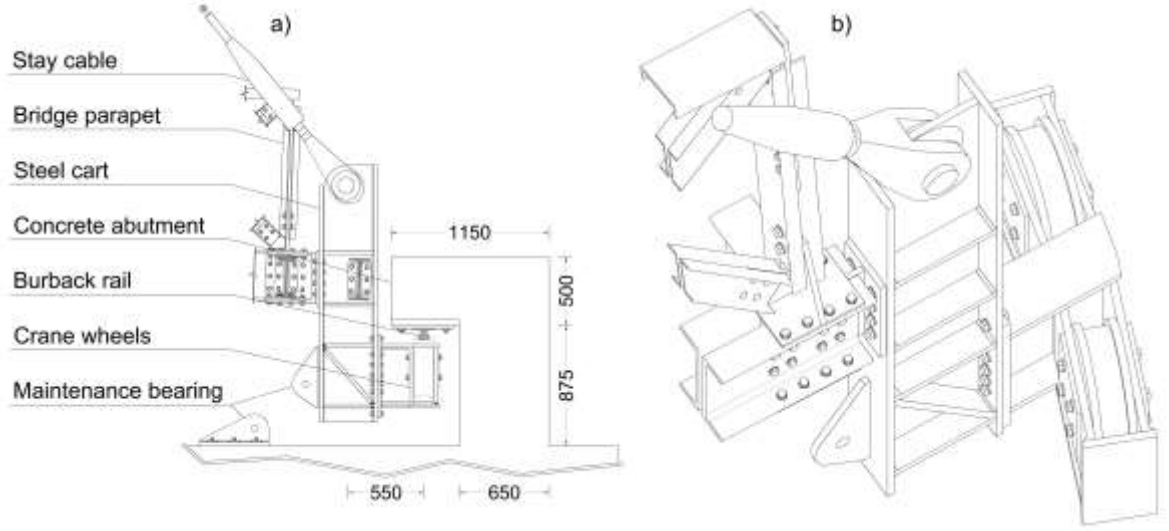

Fig. 20. Cart with crane wheels and Burback rail: (a) lateral view; (b) 3D view.

6. Cost analysis

Table 8 summarises a preliminary cost analysis for the bridge based on the estimated material quantities and current market prices [28]. The total expected construction cost turns out to be € 221,398.17. For comparison, the regional guidelines of Tuscany [42] report an average cost of € 2,300/m^2 for fixed footbridges made of traditional materials (wood, steel, and steel-concrete). Given an area of 26.64 m x 2.5 m = 66.6 m^2, the estimated cost for a traditional footbridge would be € 153,180.00. However, this amount does not include the costs for deep foundations (here, € 7,801.50 + € 8,809.71 = € 16,611.21), machinery (€ 55,306.72), expensive optional finishing (polycarbonate panels, € 12,745.66), and access ramps (€ 6,772.74). By subtracting such costs, the cost estimate for the hybrid FRP-steel bridge is € 129,961.84, about 15% less than for the traditional footbridge. The comparison would be even more in favour of the proposed FRP solution considering that installation and operational costs for the swinging mechanism would be lower than for a heavier traditional footbridge. Moreover, the maintenance works during the lifetime of the structure will be less expensive than for a traditional bridge, because of the higher durability of the FRP solution.

In particular, the FRP deck and the stainless steel elements will not require anti-corrosion measures, such as periodical painting, that would be needed by a traditional footbridge made of steel.

Table 8

Cost estimate.

Category	Work	Cost (Euro)	Cost per category (Euro)	(%)
Foundations	Excavation	375.92		
	Blinding	687.73		
	Reinforced concrete	23,141.76		
	Micropiles	7,801.50		
	Sheet pile walls	8,809.71	40,816.62	18.4
Structures	GFRP	48,416.12		
	Stainless steel (plates and bolts)	18,366.14		
	Ordinary steel (tower)	10,628.83		
	Bearings	3,622.24		
	Steel cables and anchorages	21,669.34	102,702.67	46.4
Machinery	Ordinary steel (rails, etc.)	27,406.72		
	Swinging system and electric motor	15,900.00		
	Control cabin	12,000.00	55,306.72	25.0
Finishing	Polycarbonate panels (parapets)	12,745.66		
	Aluminium waterspouts and flashings	1,500.00		
	Resin road pavement	1,553.76		
	Access ramps	6,772.74	22,572.16	10.2
	Grand total	**221,398.17**	**221,398.17**	**100.0**

7. Structural monitoring

The proposed design introduces some innovative technical solutions in the construction stages. Therefore, it is advisable to set up a structural monitoring system to verify the design hypotheses and to assess the bridge behaviour at the time of construction – in particular, during the stringing operations – and periodically under service.

During the stringing operations, the following conditions should be fulfilled:

1. the vertical deflections of the deck shall match the designed curvilinear axis at the expected values of axial force in cables;
2. the horizontal deflection of the top of the tower shall be close to zero.

After completing the construction phase, the following checks are suggested:

3. the displacements and strains under self-weight and test loads should be in line with the values predicted by the FEM model;

4. the dynamic behaviour of the structure – in particular, its natural frequencies and mode shapes – shall be similar to the one predicted by the model in both the open and closed configurations.

   During periodic inspections, the following issues should be checked:

5. the incremental displacements and strains (with respect to the construction phase) shall be minimal and similar to the ones predicted for viscous phenomena;
6. the dynamic behaviour of the structure shall not deviate significantly from the one measured at the time of construction (to ensure the lack of hidden damages and to avoid aeroelastic buckling and other dangerous dynamical phenomena).

7. 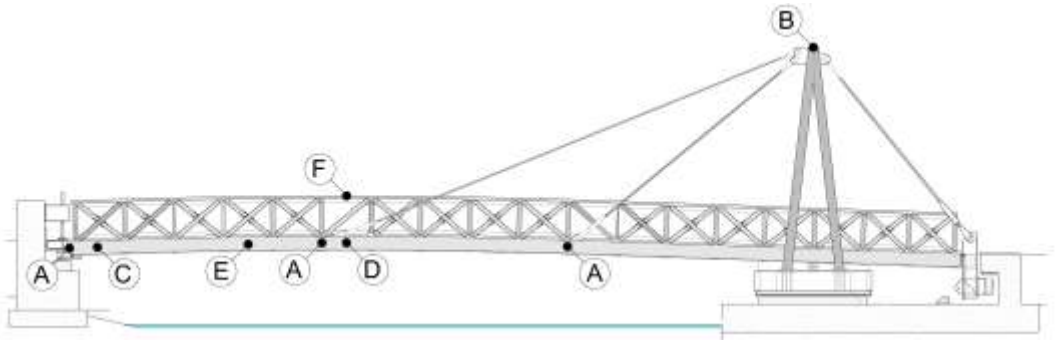

8. **Fig. 21.** Check points for structural monitoring system.

Figure 21 shows a proposal for the disposition of measurement equipment. The static vertical deflections of the deck (points marked with A in the figure) and horizontal deflections of the tower (point B in the figure) can be measured by using topographic instruments. The dynamic behaviour can be investigated via accelerometers placed at the most significant points, such as the free-end of the deck (point C) in the open configuration and the middle of the deck (point D) in the closed configuration. The strains can be measured via electrical gauges placed on the main girders (point E) and in the upper chords of the parapets (point F). The abovementioned equipment shall be placed on both sides of the bridge to evaluate its torsional behaviour.

8. Conclusions

A feasibility study has been presented of an asymmetric, cable-stayed, pedestrian, swing bridge crossing the Navicelli Canal in Pisa, Italy. If built, the planned bridge would be the first example of cable-stayed swing bridge with all-FRP deck.

The proposed solution has proven to be both technically feasible and cost-effective. The cable-stayed scheme, together with the proposed cable stringing procedure, reduces the overall deformability of the structure, hence the related buckling and vibration problems. For the bridge movement, a small-sized electrical motor will be sufficient, thus demonstrating the

potential savings in installation and operational costs with respect to a movable bridge made of traditional materials. Also, maintenance costs are expected to be lower with respect to traditional solutions thanks to the high durability of FRP materials. Given the novelty of some of the proposed design choices, the installation of a structural monitoring system has been suggested.

a)

b)

Fig. 22. Rendering of the bridge: (a) view from South-West; (b) view from South-East.

Figure 22 shows some rendering images of the bridge. Although structures made of FRP pultruded profiles are generally not appealing, the aesthetics of the planned bridge is worth being appreciated.

Acknowledgements

Design information was supplied by Navicelli di Pisa S.p.A., Italy [30], and Fiberline Composites A/S, Denmark [31]. Their technical support is gratefully acknowledged.

Funding

The first Author's MSc Thesis [28] was awarded the Best Thesis Award 2016 by the *Centro Internazionale di Aggiornamento Sperimentale-Scientifico* (CIAS) [43]. Its financial support is gratefully acknowledged.

References

[1] Bank LC. Composites for Construction. Hoboken, NJ: John Wiley & Sons; 2006.

[2] Hollaway LC. A review of the present and future utilisation of FRP composites in the civil infrastructure with reference to their important in-service properties. Constr Build Mater 2010;24:2419–45, https://doi.org/10.1016/j.conbuildmat.2010.04.062.

[3] Zhao X-L, Zhang L. State-of-the-art review on FRP strengthened steel structures, Eng Struct 2007;29:1808–23, https://doi.org/10.1016/j.engstruct.2006.10.006.

[4] Gholami M, Sam ARM, Yatim JM, Tahir MM. A review on steel/CFRP strengthening systems focusing environmental performance, Constr Build Mater 2013;47:301–10, https://doi.org/10.1016/j.conbuildmat.2013.04.049.

[5] Aslam M, Shafigh P, Jumaat MZ, Shah SNR. Strengthening of RC beams using prestressed fiber reinforced polymers – A review. Constr Build Mater 2105;82:235–56, https://doi.org/10.1016/j.conbuildmat.2015.02.051.

[6] Talreja R, Singh CV. Damage and Failure of Composite Materials. Cambridge, UK: Cambridge University Press; 2012.

[7] Fairuz AM, Sapuan SM, Zainudin ES, Jaafar CNA. Polymer composite manufacturing using a pultrusion process: A review. Am J Appl Sci 2014;11(10):1798–810, https://doi.org/10.3844/ajassp.2014.1798.1810.

[8] Huo R, Liu W, Wan L, Fang Y, Wang L. Experimental Study on Sandwich Bridge Decks with GFRP Face Sheets and a Foam-Web Core Loaded under Two-Way Bending. Adv Mater Sci Eng 2015; Article ID 434721:1–12, https://doi.org/10.1155/2015/434721.

[9] Tuwair H, Volz J, Elgawady MA, Mohamed M, Chandrashekhara K, Birman V. Testing and Evaluation of Polyurethane-Based GFRP Sandwich Bridge Deck Panels with Polyurethane Foam Core. J Bridge Eng 2016;1(1), Article number 04015033:1–13, https://doi.org/10.1061/(ASCE)BE.1943-5592.0000773.

[10] Smits J. Fiber-Reinforced Polymer Bridge Design in the Netherlands: Architectural Challenges toward Innovative, Sustainable, and Durable Bridges. Engineering 2016;2(4):518–527. https://doi.org/10.1016/j.eng.2016.04.004.

[11] Chróścielewski J, Miśkiewicz M, Pyrzowski Ł, Sobczyk B, Wilde K. A novel sandwich footbridge - Practical application of laminated composites in bridge design and in situ measurements of static response. Compos Part B-Eng 2017;126:153–161. https://doi.org/10.1016/j.compositesb.2017.06.009.

[12] Siwowski T, Kaleta D, Rajchel M. Structural behaviour of an all-composite road bridge. Compos Struct 2018;192:555–567 https://doi.org/10.1016/j.compstruct.2018.03.042.

[13] Siwowski T, Kulpa M, Rajchel M, Poneta P. Design, manufacturing and structural testing of all-composite FRP bridge girder. Compos Struct 2018;206:814-827. https://doi.org/10.1016/j.compstruct.2018.08.048.

[14] Pyrzowski Ł, Miśkiewicz M. Modern GFRP Composite Footbridges. In: Čygas D, editor. 10th International Conference on Environmental Engineering (10th ICEE) (Vilnius, Lithuania, 27–28 April 2017). Vilnius: Vilnius Gediminas Technical University; 2017, https://doi.org/10.3846/enviro.2017.143.

[15] Keller T. Recent all-composite and hybrid fibre-reinforced polymer bridges and buildings. Progr Struct Eng Mat 2001;3:132–40, https://doi.org/10.1002/pse.66.

[16] GangaRao VSH, Siva RVH. Advances in fibre-reinforced polymer composite bridge decks. Progr Struct Eng Mat 2002;4:161–168, https://doi.org/10.1002/pse.113.

[17] Bank LC. Application of FRP Composites to Bridges in the USA. In: Yamada S, editor. Proceedings of the International Colloquium on Application of FRP to Bridges (ICAFB2006) (Tokyo, Japan, 20 January 2006). Tokio: Japan Society of Civil Engineers; 2006, p. 9–16.

[18] Cheng L, Karbhari VM. New bridge systems using FRP composites and concrete: A state-of-the-art review. Progr Struct Eng Mat 2006;8:143–54, https://doi.org/10.1002/pse.221.

[19] Robinson MJ, Kosmatka JB. Development of a Short-Span Fiber-Reinforced Composite Bridge for Emergency Response and Military Applications. J Bridge Eng 2008;13(4):388–97, https://doi.org/10.1061/(ASCE)1084-0702(2008)13:4(388).

[20] Teixeira AMAJ, Pfeil MS, Battista RC. Structural evaluation of a GFRP truss girder for a deployable bridge. Compos Struct 2014;110:29–38, https://doi.org/10.1016/j.compstruct.2013.11.014.

[21] Yeh F-Y, Chang K-C, Sung Y-C, Hung H-H, Chou C-C. A novel composite bridge for emergency disaster relief: Concept and verification. Compos Struct 2015;127:199–210, https://doi.org/10.1016/j.compstruct.2015.03.012.

[22] Bai Y, Keller T. Modal parameter identification for a GFRP pedestrian bridge. Compos Struct 2008;82(1):90–100, https://doi.org/10.1016/j.compstruct.2006.12.008.

[23] Votsis RA, Stratford TJ, Chyssanthopoulos MK. Dynamic Assessment of a FRP Suspension Footbridge. In: Halliwell S, Whysall C, Stratford T, editors. Advanced Composites in Construction (ACIC 2009) (Edinburgh, UK, 1–3 September 2009). Chesterfield: NetComposites Ltd; 2009, p. 144–55.

[24] Cadei J, Stratford T. The design, construction and in-service performance of the all-composite Aberfeldy footbridge. In: Shenoi RA, Moy SSJ, Hollaway LC, editors. Advanced Polymer Composites for Structural Applications in Construction (ACIC 2002) (Southampton, UK, 15–17 April 2002). London: Thomas Telford; 2002, p. 445–53.

[25] Clarke JL, editor. Structural Design of Polymer Composites – EUROCOMP Design Code and Handbook. London: E & FN Spon; 1996.

[26] CNR-DT 205/2007. Istruzioni per la Progettazione, l'Esecuzione ed il Controllo di Strutture realizzate con Profili Pultrusi di Materiale Composito Fibrorinforzato (FRP). Rome: National Research Council;

2008.

[27] DIBt Z-10.9-299. Allgemeine bauaufsichtliche Zulassung: Pultrudierte Profile aus glasfaserverstärkten Kunststoffen; Doppel-T-Profil, U-Profil, Winkelprofil, Vierkanthohlprofil, Flachprofil und Handlaufprofil. Berlin: Deutsches Institut für Bautechnik; 2014.

[28] Alocci C. Progetto di una passerella ciclo-pedonale mobile in materiale composito sul canale dei Navicelli a Pisa (MSc Thesis). Pisa: University of Pisa, available: <https://etd.adm.unipi.it/theses/available/etd-02032016-230111/>; 2016 [accessed 15.07.2018].

[29] Wikipedia. Canale dei Navicelli, available: <https://it.wikipedia.org/wiki/Canale_dei_Navicelli>; 2018 [accessed 15.07.2017].

[30] Navicelli di Pisa S.p.A., available: <http://www.navicelli.it/> [accessed 15.07.2018].

[31] Fiberline Composites A/S, available: <https://fiberline.com/> [accessed 15.07.2018].

[32] EN 13706-2:2002. Reinforced plastics composites – Specifications for pultruded profiles – Part 2: Methods of test and general requirements.

[33] Dischinger F. Hängebrücken für schwerste Verkehrslasten. Bauing 1949;24(3):65–75 and 24(4):107–13.

[34] Ernst HJ. Der E-modul von Seilen unter Berücksichtigung des Durchhanges. Bauing 1965;40(2):52–5.

[35] Croce P. Non-linear behavior of heavy stays. Int J Solids Struct 2013;50(7–8):1093-107, https://doi.org/10.1016/j.ijsolstr.2012.12.012.

[36] Computers & Structures Inc. SAP2000, available: <https://www.csiamerica.com/products/sap2000> [accessed 15.02.2019].

[37] EN 1991-2:2003. Eurocode 1: Actions on structures – Part 2: Traffic loads on bridges.

[38] NTC 2008. D.M. LL.PP. 14/01/2008. Norme tecniche per le costruzioni.

[39] AASHTO. Guide Specifications for the Design of FRP Pedestrian Bridges. Washington: American Association of State Highway and Transportation Officials; 2008.

[40] CNR-DT 207/2008. Istruzioni per la valutazione delle azioni e degli effetti del vento sulle costruzioni. Rome: National Research Council; 2009.

[41] EN 1991-1-4:2010. Eurocode 1: Actions on structures – Part 1-4: General actions – Wind actions.

[42] Regione Toscana. Piste ciclabili in ambito fluviale – Manuale tecnico, Seconda edizione. Florence: Centro Stampa Giunta Regione Toscana; 2011.

[43] CIAS – Centro Internazionale di Aggiornamento Sperimentale-Scientifico. Esiti del Bando 2016, available: <http://www.cias-italia.it/PREMIAZIONE%20BANDO%202016.pdf> [accessed 15.07.2018].